Journal of Radiological Science and Technology, 45(2), 145-150 ISSN 2384-1168(On-line) ISSN 2288-3509(Print)

<원저>

Analysis on Optimal Approach of Blind Deconvolution Algorithm in Chest CT Imaging

Young-Jun Lee[1]·Jung-Whan Min[2]

[1]*Department of Radiology, Researcher, The Seoul National University Hospital of Korea*
[2]*Department of Radiological Technology The Shingu University of Korea*

흉부 컴퓨터단층촬영 영상에서 블라인드 디컨볼루션 알고리즘 최적화 방법에 대한 연구

이영준[1]·민정환[2]

[1]서울대병원 영상의학과·[2]신구대학교 방사선과

Abstract The main purpose of this work was to restore the blurry chest CT images by applying a blind deconvolution algorithm. In general, image restoration is the procedure of improving the degraded image to get the true or original image. In this regard, we focused on a blind deblurring approach with chest CT imaging by using digital image processing in MATLAB, which the blind deconvolution technique performed without any whole knowledge or information as to the fundamental point spread function (PSF). For our approach, we acquired 30 chest CT images from the public source and applied three type's PSFs for finding the true image and the original PSF. The observed image might be convolved with an isotropic gaussian PSF or motion blurring PSF and the original image. The PSFs are assumed as a black box, hence restoring the image is called blind deconvolution. For the 30 iteration times, we analyzed diverse sizes of the PSF and tried to approximate the true PSF and the original image. For improving the ringing effect, we employed the weighted function by using the sobel filter. The results was compared with the three criteria including mean squared error (MSE), root mean squared error (RMSE) and peak signal-to-noise ratio (PSNR), which all values of the optimal-sized image outperformed those that the other reconstructed two-sized images. Therefore, we improved the blurring chest CT image by using the blind deconvolutin algorithm for optimal approach.

Key Words: Blind Deblurring, Deconvolution, Chest CT Imaging, Gaussian Blurring, Point Spread Function (PSF)
중심 단어: 블라인드 디블러링, 디컨볼루션, 흉부 컴퓨터단층촬영 영상, 가우시안 잡음, 점확산함수

Ⅰ. Introduction

Recently, the increased frequency of using computed tomography (CT) in clinical routine has caused a higher increase in patient radiation dose [1]. Especially, chest CT examinations have been considerably increased in clinical centers and linked to the radiation dose. To diminish the exposure risk, several developed techniques reducing radiation dose have been advanced and are mounted to CT devices for clinical practice [2-5]. One of the methods is an iterative reconstruction (IR) that is currently employed to decrease the CT radiation exposure and to decline noise and blurring on the CT image. However, the approach would have limitations

Corresponding author: Young-Jun Lee, Department of Radiology, Researcher, The Seoul National University Hospital of Korea, 101, Daehak-ro, Ihwa-dong, Jongno-gu, Seoul, 03080, Republic of Korea / Tel: +82-2-2072-0141 / E-mail: qpal586@naver.com
Received 8 March 2022; Revised 27 March 2022; Accepted 4 April 2022

in clinical routine so the blind deconvolution method might complement the shortcomings in different way [6-10].

Nowadays, many blind deblurring algorithms associated with deep learning (DL) have been developed and released. DL would be useful in learning to map the blur kernel. A recent study by Schuler et al. designed the deep learning model for estimating the blur kernel [11]. In addition, deep convolutional neural architectures might predict the Fourier coefficients by investigating the property of blurring images in clinical routine [12]. And the deep network was capable of project calculating the blur kernel. In this regard, the deep convolutional neural network is possible to consider several parameters of blur kernels related to motion blurring on the clinical image [13].

In general, blind deblurring in clinical practice is to find out a blurry or degraded image without requiring prior methods linked the point spread function (PSF) or utilizing only partial details about the PSF. Recently, blind deconvolution systems were reported by previous works which indicated that there are many motivations for using blind restoration in clinical imaging applications such as general X-ray and CT [14,15]. Hence, blind restoration could be helpful for enhancing medical images quality with no complicated estimation techniques.

Before applying diverse deep learning algorithms, our work aims to analyze the blurring effect on the chest CT images and restore the true image and the PSF in person without any clinical information related to the original PSF. The demanding task of reconstructing chest CT images according to blind deconvolution has been accepted as one of the main problems in clinical chest CT imaging [16]. Our study tried to make the blurring chest CT images to be the original image through the blind deconvolution technique and to advance the restored image by using the weighted function.

II. Material & Method

1. Deblurring Images Using the Blind Deconvolution Algorithm

Data used in this paper originated from the public source (known as Kaggle) and 30 images was conducted for the performance. A blind deconvolution algorithm used in this work would be especially helpful in this circumstance where there is no known information with respect to the deformation by blurring and noise [12]. Under this condition, the algorithm enables to restore the original image and the point spread function (PSF) concurrently. For advancing the chest CT image, this study was done in MATLAB R2021a and all the data was acquired from the public source. For analyzing the blind deconstructed images, we estimated three types of criteria like mean squared error (MSE), root mean squared error (RMSE) and peak signal-to-noise ratio (PSNR) between the original image and the deblurred image to measure performance and accuracy. Several input parameters concerning the optical system were used to better the condition of the image restored. The steps of applying the blind deconvolution algorithm are followed by Fig. 1.

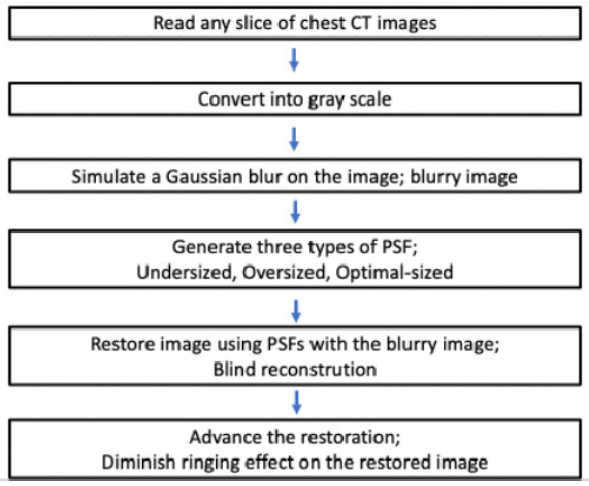

Fig. 1. Six-step blind deconvolution scheme.

2. Blind Deconvolution Definition with Gaussian Noise

The following term related to the blind deconvolution

is used in clinical imaging applications:

$$g(x) = p(x) \otimes \lambda(x) + n(x) \qquad \text{eq.1}$$

Where g(x) is the observed chest CT image, p(x) defines the imaging system and is known as the point spread function (PSF), which means the 2D convolution operator, n(x) is the specific noise term called as additive white gaussian noise with standard deviation parameter σ, and λ(x) is the original or true image. A calculation of the original image is called a reconstructed/restored/deblurred image (Fig. 2).

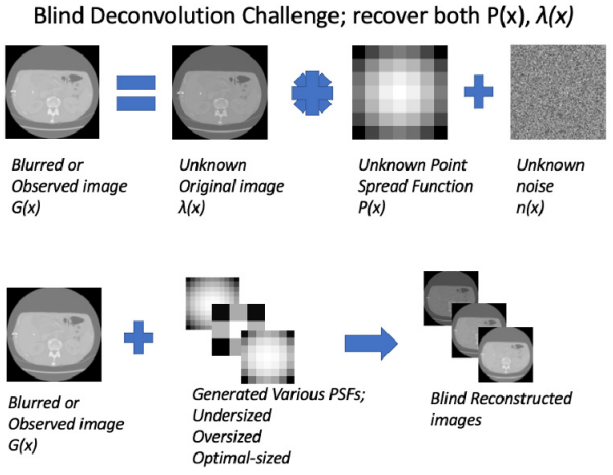

Fig. 2. Blind deconvolution logic and approximation of original imageg(x) and point spread function p(x) from the blurry image λ(x) with using varied point spread functions.

In summary, the observed image or blurry image g(x) is distorted with certain noise such as additive white gaussian noise, which is designed as an assembly of random variables by indexing the spatial variable x with means values g(x). And the gaussian noise is one of the varied types of noise widely used in clinical imaging such as gaussian, passion and rician. Furthermore, according to the central limit theories, the net outcome of the complicated interaction out of those independent random variables could be estimated by the gaussian PSF with standard deviation factor σ:

$$G_\sigma(x) = \frac{1}{2\prod\sigma^2} e^{-\frac{x^2}{2\sigma^2}} \qquad \text{eq.2}$$

Ⅲ. Result & Discussion

Step 1: Read any slices related to chest CT examinations into the workplace, using the functions; 'dicomread' and 'rescale' (Fig. 3).

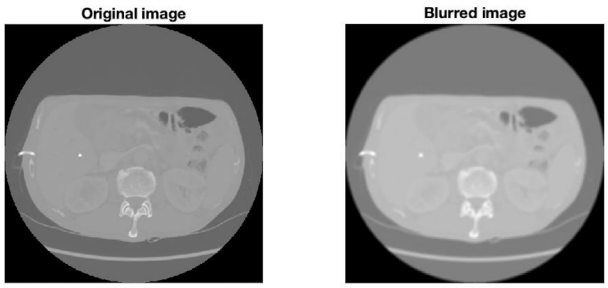

Fig. 3. Original chest CT images converted into gray scale as an original or true image (Left) and the blurred image with Gaussian noise (Right)

Step 2: The image simulated by some noise and blurring linked to the patient movement or larger inspiration during the scanning, creating a point spread function (PSF) akin to the blurring by performing the motion filter. The Gaussian noise filter represents the PSF related to blurring, combining the PSF with the original image (Fig. 3).

Step 3: To restore the blurred chest CT image to the original image and find out the optimal PSF size and shape for the satisfactory result, we reconstructed the PSF each time as performing three restorations.

1. Lower-sized PSF

The first restoration was computed from a lower-sized array for an initial estimation, which is 4 pixels shorter in the fourth dimension than the original PSF (Fig. 4).

2. Over-sized PSF

The result of the second restoration was based on

an array of ones and the over-sized PSF that extend 4 pixels ineach dimension than the original PSF (Fig. 4)

3. Approximated optimal-sized PSF

The final restoration as a third was similar to the original PSF in terms of the value and size, using an array of ones (Fig. 4).

Step 4: Analysis of the three restorations with PSFs

Three restorations generated a PSF each iterative time: undersized PSF, oversized PSF, optimal-sized PSF. The following figures mean that the restored PSFs would support predicting the optimal size for the initial PSF. The pixel's value is brighter because the location of the maximum values was close to the central. Conversely, the farther away the border values are diminished from the center and changed to black (Fig. 4). In addition, the result of the deblurred image with the optimal-sized PSF estimated outperformed the other deconstructed images all out of three performance assessments. The mean value of the optimal-sized PSF pertaining the MSE criteria was fairly lower than other results and the quality of the image could be similar to that of the true image since the shape of the PSF was be close to that of the original PSF. For the over-sized PSF, all mean values of three criteria was more poor than other-sized PSFs because the PSF's array might be dense, which would result in the ringing effect (Table 1).

The first PSF reconstructed to the undersized size did not correspond to the original PSF signal owing to the strong signal variance at the boundary. As figure 4 shown, the image depending on the first PSF was not improved in terms of blurring and noise, compared

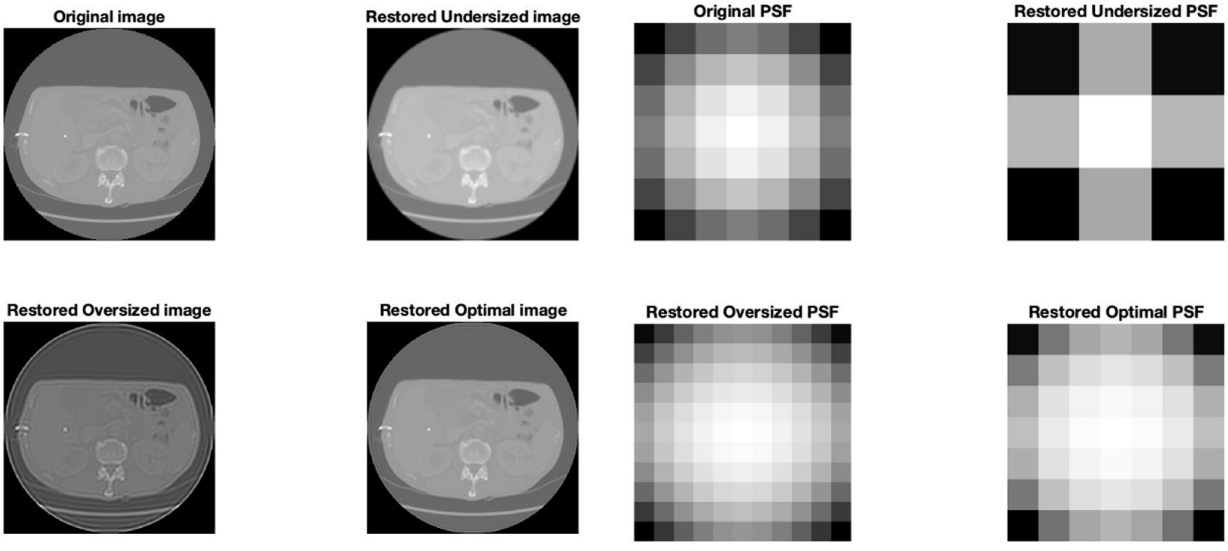

Fig. 4. Comparison between the original image and the restored images with various point spread functions: under-sized, over-sized and optimal-sized PSF

Table 1. Comparison based on various performance metrics such as MSE, RMSE and PSNR between the original image and the deblurred images

Blind Reconstruction	MSE	RMSE	PSNR
Deblurred image with under PSF	6.8842 ± 5.02	0.0262 ± 4.59	31.6214 ± 6.09
Deblurred image with over PSF	37.0000 ± 10.27	0.0611 ± 5.23	24.1871 ± 9.56
Deblurred image with optimal PSF	2.4053 ± 4.90	0.0157 ± 2.11	36.1079 ± 4.11

to the original image. The over-sized PSF restoration became smooth at the boundary, which the corresponding image means strongly disrupted by the ringing artifact. The PSF result from the third restoration appeared the intermediate condition between the first PSF and the second PSF. Particularly, the array of the PSF was similar to that of true PSF, and the third reconstructed image accorded with the PSF indicated advanced conditions, contrary to the others. Yet, the third image was still distorted a little by the ringing artifact.

Step 5: Diminishing the ringing effect

The distortion known as a ringing artifact in the third restoration appeared surrounding the sharp enhancement and along the boundary. Considering this factor, applying a weighting function on the reconstructed image could be effective for diminishing the ringing effect, which shows that each pixel on the image was weighted depending on the weight array reconstructing the image and the PSF. The iteration of weighted function is approximately 30 times and used to sobel fiter. Forthermore, a combination of edge detection function and morphological processing was used to find the sharp pixels. By convolving the third restoration with the weight array, the deblurred image seemed to suppress the ringing effect (Fig. 5).

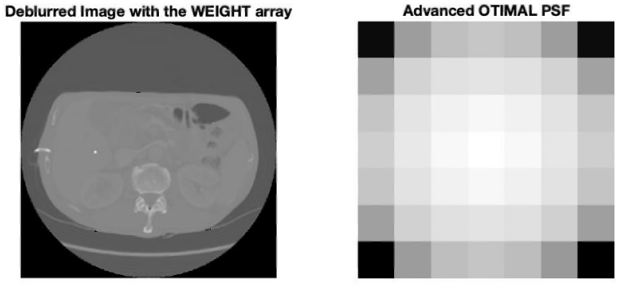

Fig. 5. The advanced image and point spread function declined the ringing effects by using weighted arrays.

In general, chest CT axial images consisted of complicated data combinations, which could be described in terms of speckle information. Depending on visual inspection, speckle noise is constituted with a comparably high gray scale enhancement, ranging between bright (hyper-echoic) and dark (hypo-echoic) domains. Furthermore, chest CT images have some benefits of being time-saved, non-invasive and relatively low cost than MRI. In this regard, our approach focused on reducing noise and blurring without diagnostic information loss for high quality and condition on the images by using various filtering algorithms. Therefore, this work was to research the optimal point spread function (PSF) value on the chest CT axial image and make the image better.

However, this work has several limitations. One of the limitations is the data quantity used from this paper since the chest CT image originally might be sensitive to obtain from the hospital such as IRB acquisition. Under this condition, this method and result both were based on public sources and the quality and value of the image were similar to that of the hospitals. Although the size of data applied from this work was not enough and satisfactory, the performance of the blind deconvolution algorithm was better depending on previous reports [17-18]. Our results was derived from 30 chest CT images in public sources. And the iteration applied the weighted function was 30 times but its times might be different depending on types of image. Further research should be based on enough volume of data for robustness and high accuracy in investigating and studying. Lastly, we hope that this approach and knowledge would be widely spread out and applied to the society of radiological technologists [19-20].

Ⅳ. Conclusion

Our experimental work aimed to analyze the enhancement of the chest CT image and to estimate the original image and the true PSF by using the blind deconvolution algorithm, ultimately which means to decline the noise and blurring on the chest CT image.

REFERENCES

[1] Fokkens WJ, Lund VJ, Mullol J, Bachert C, Alobid I, Baroody F, et al. EPOS 2012: European position paper on rhinosinusitis and nasal polyps 2012. A Summary for Otorhinolaryngologists. Rhinology. 2012;50(1):1-12.

[2] Goo HW. CT radiation dose optimization and estimation: An update for radiologists. Korean Journal of Radiology. 2012;13(1):1-11.

[3] Gunn ML, Kohr JR. State of the art: Technologies for computed tomography dose reduction. Emergency Radiology. 2010;17(3):209-18.

[4] Kalra MK, Maher MM, Toth TL, Hamberg LM, Blake MA, Shepard JA, et al. Strategies for CT radiation dose optimization. Radiology. 2004;230(3):619-28.

[5] McCollough CH, Bruesewitz MR, Kofler Jr. JM. CT dose reduction and dose management tools: Overview of available options. Radiographics. 2006;26(2):503-12.

[6] Beister M, Kolditz D, Kalender WA. Iterative reconstruction methods in X-ray CT. Physica Medica. 2012;28(2):94-108.

[7] Fleischmann D, Boas FE. Computed tomography-old ideas and new technology. European Radiology. 2011;21(3):510-7.

[8] Kalra MK, Woisetschl ger M, Dahlstr m N, Singh S, Lindblom M, Choy G, et al. Radiation dose reduction with sinogram affirmed iterative reconstruction technique for abdominal computed tomography. Journal of Computer Assisted Tomography. 2012;36(3):339-46.

[9] Leipsic J, Heilbron BG, Hague C. Iterative reconstruction for coronary CT angiography: Finding its way. The International Journal of Cardiovascular Imaging. 2012;28(3):613-20.

[10] No l PB, Fingerle AA, Renger B, M nzel D, Rummeny EJ, Dobritz M. Initial performance characterization of a clinical noise-suppressing reconstruction algorithm for mdct. American Journal of Roentgenology. 2011;197(6):1404-9.

[11] Schuler CJ, Hirsch M, Harmeling S, Sch lkopf B. Learning to deblur. IEEE Transactions on Pattern Analysis and Machine Intelligence. 2015;38(7):1439-51.

[12] Chakrabarti A. ed. A neural approach to blind motion deblurring. European Conference on Computer Vision. Springer; 2016.

[13] Sun J, Cao W, Xu Z, Ponce J. eds. Learning a convolutional neural network for non-uniform motion blur removal. Proceedings of the IEEE Conference on Computer Vision and Pattern Recognition. 2015.

[14] Kundur D, Hatzinakos D. Blind image deconvolution. IEEE Signal Processing Magazine. 1996a;13(3):43-64.

[15] Kundur D, Hatzinakos D. Blind image deconvolution revisited. IEEE Signal Processing Magazine. 1996b;13(6):61-3.

[16] Chae KJ, Goo JM, Ahn SY, Yoo JY, Yoon SH. Application of Deconvolution Algorithm of Point Spread Function in Improving Image Quality: An Observer Preference Study on Chest Radiography. Korean J Radiol. 2018;19(1):147-152.

[17] Kaushik P, Chawla M, Kumar G. Detection of Noise in an Image using Blind Deconvolution Method. International Journal of Scientific Research and Management. 2020;3:3411-5.

[18] Sharma K, Kundra S. Restoration of Medical Images using Blind Image Deconvolution based on Ant Colony. International Journal of Computer Applications. 2013;84:24-7.

[19] Lee YJ, Min JW. Comparison of Based on Histogram Equalization Techniques by Using Normalization in Thoracic Computed Tomography. Journal of Radiological Science and Technology. 2021;44(5):473-80.

[20] Min JW, Jeong HW. Evaluation of Resolution Characteristics by Using Chart Device Angle. Journal of Radiological Science and Technology. 2021;44(4):375-80.

구분	성명	소속	직위
제1저자, 교신저자	이영준	서울대병원 영상의학과	연구원
공동저자	민정환	신구대학교 방사선과	부교수